International Journal of Pavement Research and Technology
https://doi.org/10.1007/s42947-023-00398-5

社團法人中華鋪面工程學會
Chinese Society of Pavement Engineering

ORIGINAL RESEARCH PAPER

Statistical Assessment of Different Aggregate Shape Factors

Sathushka Heshan Bandara Wijekoon[1,2] · **Daniel Niruban Subramaniam**[2] · **Navaratnarajah Sathiparan**[2]

Received: 1 July 2023 / Revised: 31 October 2023 / Accepted: 2 November 2023

Abstract

This study aims to investigate aggregate geometric characteristics and analyze the possible aggregate shape factors on their statistical relationships. The study used 2192 crushed rock particles from 5 to 30 mm in diameter for the investigation. The particles were milled in a ball mill at 0, 1000 and 2000 revolutions to obtain different morphological aspects. The milled aggregate was taken and digital image processing techniques were used to obtain images and data of the aggregate which represent the 14 different shape aspects. The obtained data were statistically analyzed using data analysis tools and represented the statistical relationships. These statistical classifications can be useful for researchers to optimize the performance of aggregate mixtures in different morphological shape aspects.

Keywords Aggregate shape factors · Circularity · Sphericity · Solidity · Aspect ratio

1 Introduction

1.1 Background

Concrete is a heterogeneous material, and its mechanical behavior and durability are significantly influenced by its composition. To comprehend the primary factors governing its properties, it is crucial to investigate its composition and behavior [1]. In contrast, concrete is a composite of hydraulic cement, aggregates, and water, optionally enhanced with admixtures, fibers, or other cementitious materials. Coarse aggregates are vital in concrete quality, since they constitute 40–60% of the concrete volume [2]. Moreover, aggregates exhibit chemical reactivity and can interact with the cement paste, profoundly impacting the final concrete properties. These properties, in turn, depend on the geometric and textural parameters of the aggregates. Geometric parameters include particle count, area fraction, size distribution, shape characteristics, spatial distribution and more [3].

Properly graded coarse aggregates result in denser concrete, reduced void ratio, and increased packing density. Most concrete mix proportioning standards define aggregates as angular and rounded. It has been established that the shape and texture of aggregate particles exert a significant influence on concrete properties, encompassing strength, workability, and durability [1, 4–10]. If one seeks to optimize concrete mixtures for specific applications, it is imperative to comprehensively evaluate the influence of aggregate shape and texture, as understanding their impact is essential for achieving desired concrete performance and characteristics.

Aggregate shape analysis in concrete mixtures relies on assessing the geometric properties of aggregate particles, a task often accomplished through digital image processing (DIP). DIP facilitates automated characterization of aggregate shape, with various techniques available, including X-ray tomography, laser profiling, and photo geometry [11]. While most DIP methods generate two-dimensional (2D) images of aggregates, some researchers have managed to capture the third dimension through orthogonal views to measure aggregate volume [12]. However, it is worth noting that most DIP techniques primarily facilitate the determination of parameters, such as faction and not volume or weight, thereby making it challenging to quantify shape characteristics in terms of mass or volume. Consequently, when assessing aggregate shape factors in concrete, it is vital to recognize DIP techniques' inherent limitations and capabilities for accurate analysis and characterization [13, 14].

✉ Sathushka Heshan Bandara Wijekoon
sathushkahesh@hotmail.com

1 Faculty of Graduate Studies, The University of Jaffna, Thirunelvely, Jaffna 40000, Sri Lanka

2 Department of Civil Engineering, The University of Jaffna, Ariviyal Nagar, Kilinochchi 44000, Sri Lanka

Numerous studies in aggregate characterization using digital image processing (DIP) methods have been conducted by previous researchers, particularly to discern shape factors capable of modeling and predicting the packing properties of concrete, as exemplified by Das [11]. In the most recent investigation, Gucluer [15] delved into the impact of aggregate textural attributes on key concrete properties, specifically compressive strength and ultrasonic pulse velocity (UPV). By employing two distinct aggregate types and employing image analysis methods to quantify parameters, such as aspect ratio, roundness, length, and the total cross-sectional area, Gucluer's research unveiled a notable trend: an increase in aggregate surface roughness correlated with elevated concrete compressive strength and ultrasonic pulse velocity.

Similarly, the work of Mora and Kwan [16], brought the focus to sphericity, shape factor, and convexity factors in concrete, utilizing DIP techniques for analysis. Their comprehensive data analysis aimed to establish connections between these shape parameters and the conventional measures of angularity. The results revealed several shape parameters exhibiting a strong correlation with traditional measures of angularity. However, it was noteworthy that, based on their findings, only the convexity and fullness ratios proved suitable for angularity assessment. Further research by Mora and Kwan challenged the conventional perspective, suggesting that traditional angularity measures in terms of packing density should be discarded, emphasizing that packing density is indeed a crucial indicator of aggregate performance but falls short as a reliable measure of angularity.

Ozen and Guler [17] identified the significance of determining the maximum ferret diameter as the most suitable shape parameters for estimating aggregate size distribution, particularly when computed based on the diagonal sieve opening. Their research culminated in developing an algorithm that successfully identified distribution functions, ultimately leading to calculating an optimum threshold for precise aggregate shape parameter detection.

In addition to the above contributions, numerous researchers, such as Barksdale et al., Li et al., Yue and Morin., Kuo et al., Lewis and McConchie., Kim et al., Xu and Guida., Zhang, et al., etc., have harnessed DIP techniques to investigate morphological characteristics of aggregates. Their collective efforts have yielded a diverse array of shape factors tailored to model and predict the influence of particle shape and texture on concrete mixtures. These findings have significantly enriched our understating of the role of aggregate characteristics in concrete performance and have laid the groundwork for more precise and informed concrete mixture design.

In this research, we have undertaken a systematic exploration of aggregate shape factors that were identified through a comprehensive literature review. An attempt has been made to deeply analyze the identified shape factors using statistical methods to understand their statistical relationships and their morphological aspects that are quantified by them.

The significance of this study lies in its potential to offer valuable insights to researchers and practitioners working in the field of concrete technology and design by unraveling the intricate statistical relationships of these shape factors.

This research is a vital resource, providing a foundation for researchers and practitioners to build their concrete mix designs. By understanding the impact of aggregate shape, they can develop more informed and tailored concrete formulations. In addition, findings will help to engineer concrete with optimized properties, aligning with the specific requirements of various applications and ensuring that the influence of aggregate shape is systematically considered in the design process.

2 Materials and Methods

2.1 Testing Program

For this investigation, crushed aggregates were used as the raw materials, and aggregates were obtained from local quarries. The typical aggregate size used for this research is 5–30 mm in diameter. Samples of aggregate selected from the segregated range were divided into three groups. The selected samples undergo the Los Angeles Abrasion (LAA) test as per the ASTM C131 to make them smooth and, change the shape of the particle significantly. Three groups of aggregates were processed using LAA in three different revolutions (0, 1000 and 2000). After the revolutions were completed each sample was taken out and sieved with 30 mm (passes) and 5 mm (retain) sieves and segregated particle size within the 5–30 mm size range. The segregated particles were washed using clean water and left to air dry in the room environment for 24 h.

To use image analysis technics, a specific number of aggregates were taken from each sample and colored in black paint, and let dry at room temperature. After drying, colored particles were spread on a white A4 size paper in a special arrangement. An image of arranged particles was taken by covering the entire A4 area. For the second shot particles were mixed and re-arranged on the sheet and images were taken again. This procedure was repeated for 12 attempts and 12 different images were taken for analysis. ImageJTM software is an open-source software used to process and analyzed scientific images. The images were cropped with a completely white sheet and converted to binary scale in the software (black and white) following the scaling of the image. The binary images were processed and black zones of the binary images were obtained from the aggerate surface area as reference. The diameter of each white zones was found and a histogram was obtained through this process cumulative percentages of aggregates were found and the particle size distribution curve was plotted.

2.2 Particle Size Distribution Analysis Using Image Analysis

Particle Size Distribution (PSD) is the representation of the percentage of particles in each size bin (diameter), drawn to a cumulative percentage that passes through particular sieves. In this analysis using the image of aggregates, the area of each particle is computed individually using the image analysis tool ImageJ™, and the area-equivalent circle was drawn the diameter of which was computed and noted. The analyzed aggregate is assumed of a particle of the computed diameter.

The particles were arranged in ascending order of corresponding diameter and bins of 1 mm were then devised and the aggregates were categorized. The total area within each bin (summation of the areas of each aggregate in each bin) was computed and recorded as the percentage of the total area (sum of areas of all aggregates). The percentages of each bin were then computed as the cumulative percentage of aggregate area up to the bin in consideration (from the lowest bin diameter) and the graph was plotted against the bin diameter. The plot is the PSD of aggregates in the sample analyzed using an image analysis tool. The mean of the percentages across all repetitive samples were obtained to represent the mean PSD of the sample population of aggregates belonging to a particular group.

2.3 Computation of Shape Factors

ImageJ is a popular image processing and analysis software that allows to perform a wide range of tasks on digital images. It provides various tools and functions for image analysis, including measurements of different geometric properties, such as circularity, aspect ratio, roundness, and solidity.

Circularity: circularity is a measure of how closely an object resembles a perfect circle. A perfectly circular object will have a circularity value of 1, while irregular shapes will have values closer to 0.

Aspect ratio: aspect ratio is the ratio of an object's width to its height. It provides information about the elongation or compression of an object along a specific axis. In ImageJ, it can measure the aspect ratio by dividing the length of the longer axis by the length of the shorter axis.

Roundness: roundness is a measure of how close an object's shape is to a perfect circle. It is calculated as the reciprocal of the aspect ratio, normalized to a range between 0 and 1. A perfectly round object will have a roundness value

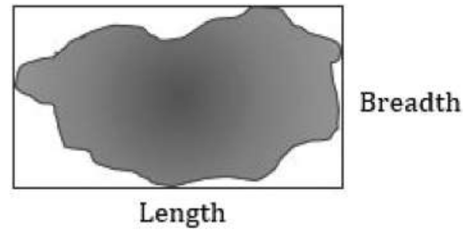

Fig. 1 Length and breadth of aggregate particle

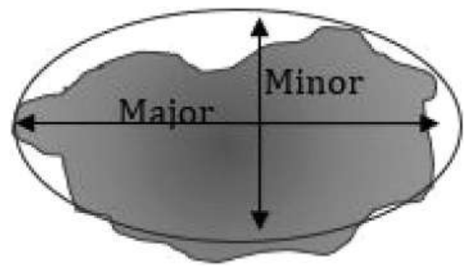

Fig. 2 Major and minor axes of an aggregate particle

of 1, while elongated or irregular shapes will have values closer to 0.

Solidity: solidity is a measure of an object's compactness or convexity. It is calculated as the ratio of the object's area to the area of its convex hull (the smallest convex polygon that completely encloses the object). Solidity provides information about how concave or convex an object's boundary is. Solidity values range from 0 to 1, where 1 indicates a completely solid and convex object.

Computational models to quantify the shape factors require the quantification of the following dimensional parameters.

Bounding rectangle—the smallest rectangle enclosing the selection. This dimension is called as breadth and height in ImageJ, as shown in Fig. 1.

Fit ellipse—the best fitting ellipse for this area. For this method, primary axis and secondary axis lengths were needed, which are shown as Minor and Major in ImageJ, as shown in Fig. 2.

Feret's dimensions—there are two Feret's dimensions. It measures the size of an area along a specified direction, as shown in Fig. 3.

Feret—the longest distance between any two points of the section boundary (Maximum Caliper).

MinFeret—the smallest distance between any two points of the section boundary (Minimum Caliper).

The following 14 different computational models employed to quantify the shape of aggregate in contemporary literature are considered for analyses in this study, the details of which are given in Table 1.

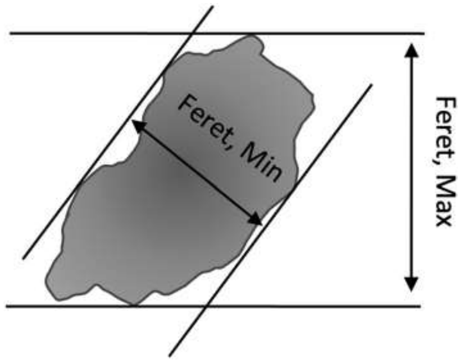

Fig. 3 Feret dimensions of an aggregate

Table 1 Shape factors used in this study

ID	Shape factor	Computation	References
IJC	ImageJ circularity	$\frac{4\pi\ area}{(\text{perimeter})^2}$	[18]
IJAR	ImageJ aspect ratio	$\frac{\text{Major axis}}{\text{Minor axis}}$	[18]
IJR	ImageJ roundness	$\frac{4\pi\ \text{area}}{\pi\times\text{major axis}^2}$	[18]
IJS	ImageJ solidity	$\frac{\text{Area}}{\text{Convex area}}$	[18]
KS	Krumbein sphericity	$\sqrt[3]{\frac{\text{Breadth}}{\text{Length}^2}}$	[19]
BSF	Barksdale et al. shape factor	$\frac{\text{Length}}{\text{Breadth}^2}$	[20]
KMFR	Kwan and Mora fullness ratio	$\sqrt[2]{\frac{\text{Area}}{\text{Convex area}}}$	[16]
SFFR	Sneed and Folk flatness ratio	$\frac{\text{Breadth}}{\text{Length}}$	[21]
FAR	Feret's aspect ratio	$\frac{\text{Feret}}{\text{MinFeret}}$	[22]
SF	Shape factor	$\frac{\text{Perimeter}}{\text{Calculated perimeter}}$	
PSC	Projected sphericity/circularity	$\frac{\text{D. calculated}}{\text{Feret}}$	[23]
ICS	Inscribed circle sphericity	$\sqrt{\frac{\text{MinFeret}}{\text{Feret}}}$	[24]
C	Circularity	$\frac{\text{Perimeter}^2}{\text{Area}}$	
PS	Projected sphericity	$\frac{\text{Area}}{\text{AC}}$	

2.4 Analytical Investigation

Number or revolutions and shape factor as two quantitative random variables can be characterized using different statistical tools. In this research Pearson correlation analysis, Principal component analysis and Clustering analysis mainly used to verify the efficiency of shape factors in characterizing the aggregate based on shape affected by the milling process.

2.4.1 Pearson Correlation Analysis

Interpreting correlation coefficients involves assessing the strength and direction of the relationship between two variables. The correlation coefficient ranges from -1 to $+1$, with a value of 0 indicating no correlation, a positive value indicating a positive correlation, and a negative value indicating a negative correlation (Fig. 4).

The strength of the correlation can be interpreted as follows:

- A value between 0 and 0.3 indicates a weak correlation
- A value between 0.3 and 0.7 indicates a moderate correlation
- A value between 0.7 and 1 indicates a strong correlation

2.4.2 Principle Component Analysis

Principal Component Analysis (PCA) is a statistical technique used to analyze and reduce the dimensionality of large data sets. It works by identifying patterns and correlations in the data and transforming the data into a smaller set of uncorrelated variables called principal components. The main objective of PCA is to identify the most important variables that contribute the most to the variation observed in the data set. These variables are then used to create new variables (principal components) that explain most of the variation in the data. The first principal component explains the largest amount of variation in the data, the second principal component explains the second largest amount of variation. When conducting a principal component analysis (PCA), the resulting output can be interpreted in several ways. PCA can also be used to reduce the dimensionality of the data set by retaining only the most important principal components. This can be useful when working with large data sets or when trying to simplify the analysis of the data.

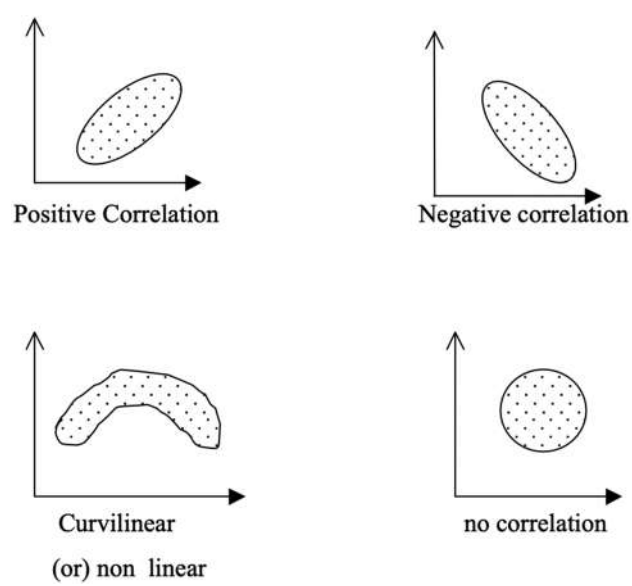

Fig. 4 Pearson correlation distributions

2.4.3 Cluster Analysis

Cluster analysis is a statistical technique used to group data points into clusters based on their similarities. The main objective of cluster analysis is to identify groups of data points that are similar to each other, and different from data points in other groups.

There are different types of cluster analysis techniques, including hierarchical clustering and k-means clustering. In k-means clustering, the data points are partitioned into a fixed number (k) of clusters based on their proximity to a pre-defined set of cluster centroids.

3 Results and Discussion

3.1 Introduction

To identify the statistical relationship of shape factors and to understand their morphological aspects, this study deeply analyzes 14 different shape factors selected from the contemporary literature. Pearson correlation analysis, Principal component analysis and Clustering analysis mainly used for analysis.

3.2 Visual Inspection of Aggregates

Figure 5 shows the pictures of randomly collected aggregates from each groups that have undergone different degrees of milling (up to 2000 revolutions), where 0 rev indicates the original crushed aggregates. It is evident from the figure that

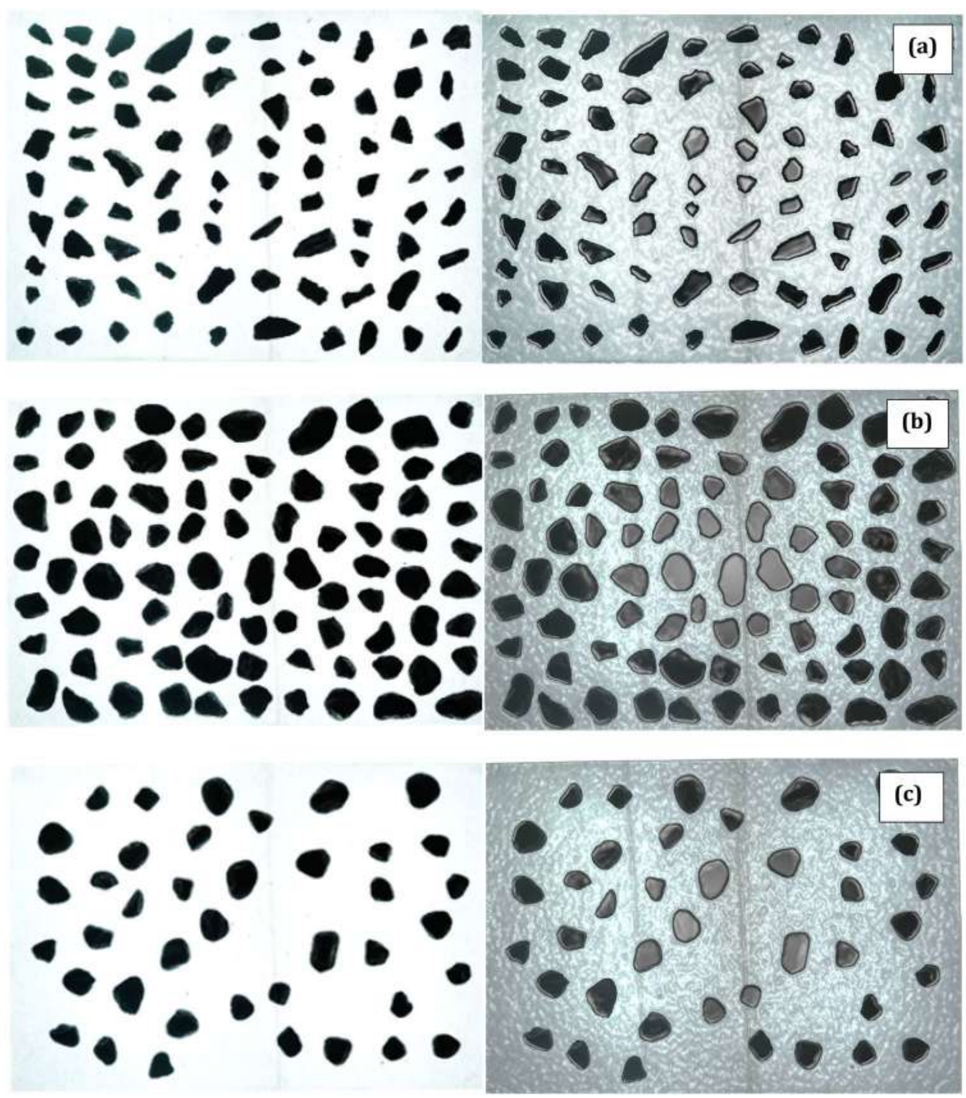

Fig. 5 Pictures of sample aggregates that have undergone varied degrees of milling, **a** 0, **b** 1000, and **c** 2000 milling

the characteristics of aggregates significantly differ between the degrees of milling, particularly, the change in texture and shape.

The surface texture relates to highly frequent irregularities on the surface of the aggregates, where the shape would be indicated by less frequent irregularities as discussed in the Fourier analysis of the aggregate image. Specifically, when the milling is more intense (prolonged), the aggregate tends to become more rounded (spherical in 3 dimensional), while a lower degree of milling corresponded to smoothing of the surface, essentially changing the texture of the aggregate surface. Shape factors may intend to quantify any or all of the changes in the shape characteristics of the aggregate ranging from texture to macro-shape. The analysis conducted to identify which of the shape factor computational models retrieved from the literature quantify the morphological change visually observed in the aggregates shown in the figure.

3.3 Descriptive Statistics of Shape Factors

Table 2 shows the descriptive statistics details of variables of aggregate characteristics analyzed in this study. Statics shows for aggregate area 50–150 mm^2 and 0, 1000 and 2000 LAA revolutions, a total of 2192 aggregate particles. It can be observed that the minimum and maximum area is 50.00 mm^2 and 149.88 mm^2. The standard deviation of the area is 26.86 and it is lesser than the mean value (82.70). The Kurtosis value used describes the shape probability and it is the measure of the "peakedness" or "flatness" of the distribution. IJR, KS, SFFR, and PS shows low peak pattern. However, C and SF shoes very high Kurtosis values which could represent sharp peak distribution. In addition, it can be observed that shape factors IJC, IJR, IJS, KS, KMFS, SFFR, PSC, ICS, and PS show negative skewness (left tail), while IJAR, BSF, FAR, SF, and C show positive skewness (right tail). Furthermore, the standard error of skewness is very low and consistent, the ratio of skewness to its standard error is within the range of $+2$ and -2. Hence, there are no concerns over the normality of the data.

Histograms of shape factors are used to observe how widely data are dispersed with the frequencies of each bin and to check the reliability of the data. As per Fig. 6, it can be recognized that IJC, IJR, IJS, KS, KMFR, PSC, and ICS shows a peak to the right of the center and more gradually tapering to the left side. Furthermore, it shows unimodal which mode is closer to the right (left-skewed) and greater than either the mean or median. In addition, the shape indicates that the preponderance of any outliers is lesser than the mode. On the other hand, IJAR, BSF, FAR, SF, SFFR, and C shows a right-skewed histogram, where the peak is left of the center and more gradual tapering to the right side of the graph. This is unimodal, with the mode closer to the left graph and smaller than either the mean or the median. Furthermore, this shape indicates that there are several data points, perhaps outliers that are greater than the mode. Shape factor PS shows a kind of bell-shaped histogram where a prominent mount in the center and similar tapering to the left and right. This unimodal shows that data have a single mode, identified by the peak of the curve. In addition, it can be considered a normal distribution.

Furthermore, three shape factors were selected from each unimodal to further investigate the data dispersed in frequencies of different milling.

As per Fig. 7, KMFR shows a similar right skewed pattern of histogram, while BSF shows left skew in 1000 and 2000 milling. PS shows a bell-shaped distribution in 1000 and 2000 millings, whereas 0 milling shows a uniform distribution.

Figure 8 shows box and whiskers plots of BSF, KMFR, and PS shape factors. The box plot of BSF and PS is fairly consistence with one from the normal distribution; the median is fairly close to the center of the box. The box plot of KMFR is slightly distributed the median is close to the upper quartile which would be suggesting a negative skewness. Furthermore, PS is with qual length of whiskers. BSF is positively skewed, because the whisker and half box are longer on the right side of the median than on the left side. All three distributions include potential outliers. These outliers affect the mean, median, and other percentiles, all 14 shape factors show outliers, where C, SF, BSF, FAR, and IJAR show outliers above the upper whisker. All other shape factors show outliers below the lower whisker.

Figure 9 shows the shape factor data vs area distribution in different millings (0, 1000 and 2000). As per observations, high revolutions result in low area aggregate area. In addition, it could be visible that high milling concentrates the distributions to a corner. IJAR, FAR, SF, and C shape factors with high milling, data concentrated to the left bottom corner (low shape factor value) while, IJC, KS, KMFR, BSF, IJS, and ICS concentrated to the right bottom corner (high shape factor value). However, SFFR, IJR, PS, and PSC shape factors show distributed patterns.

It can be concluded that some of the shape factor values are improved with high milling while the area of the aggregate gets low, while some of the factors decrease. In addition, some of the shape factors are becomes neutral.

It could observe that PSC and PS shape factors show similar distribution against all milling. PSC and ICS values lay in between 0.5 and 1.00 while PS values lay at 0.2–1.00. Furthermore, SF and C show an identical distribution where SF values lie in between 1.00 and 1.6 and C values lay in between 13 and 32.

Figure 10 shows Pearson's correlation coefficients of Perimeter (P), projected area (A), and 14 different shape factors of 50–150 mm^2 size aggregates with the milling of

Table 2 Descriptive statistics details of variables of aggregate characteristics analyzed in this study

Statistics	Perimeter (mm)	Area (mm^2)	IJC	IJAR	IJR	IJS	KS	BSF (mm^{-1})	KMFR mm$^{(1/3)}$	SFFR	FAR	SF	PSC	ICS	C	PS
N																
Valid	2192	2192	2192	2192	2192	2192	2192	2192	2192	2192	2192	2192	2192	2192	2192	2192
Missing	0	0	0	0	0	0	0	0	0	0	0	0	0	0	0	0
Mean	36.4740	82.7039	0.7669	1.3552	0.7605	0.9607	0.4196	0.1264	0.9801	0.8496	1.3789	1.1443	0.8264	0.8591	16.4809	0.6867
Median	35.1295	74.6135	0.7750	1.2920	0.7740	0.9640	0.4209	0.1201	0.9818	0.8673	1.3246	1.1359	0.8345	0.8689	16.2153	0.6963
Std. deviation	6.24737	26.86352	0.05481	0.26491	0.12004	0.01445	0.03570	0.03509	0.00742	0.10601	0.23101	0.04487	0.06124	0.06172	1.34345	0.09822
Variance	39.030	721.648	0.003	0.070	0.014	0.000	0.001	0.001	0.000	0.011	0.053	0.002	0.004	0.004	1.805	0.010
Skewness	0.628	0.747	−1.247	2.066	−0.627	−1.499	−0.543	1.569	−1.539	−0.852	2.009	2.031	−0.845	−0.987	2.417	−0.583
Std. error of skewness	0.052	0.052	0.052	0.052	0.052	0.052	0.052	0.052	0.052	0.052	0.052	0.052	0.052	0.052	0.052	0.052
Ratio—st. error of skewness/skewness	0.083	0.070	−0.042	0.025	−0.083	−0.035	−0.096	0.033	−0.034	−0.061	0.026	0.026	−0.062	−0.053	0.022	−0.090
Kurtosis	−0.530	−0.572	2.894	6.736	0.309	3.663	0.353	4.595	3.910	0.562	6.436	8.509	1.093	1.291	12.326	0.415
Std. error of kurtosis	0.105	0.105	0.105	0.105	0.105	0.105	0.105	0.105	0.105	0.105	0.105	0.105	0.105	0.105	0.105	0.105
Minimum	26.98	50.00	0.41	1.00	0.30	0.86	0.28	0.07	0.93	0.42	1.04	1.07	0.54	0.56	14.37	0.30
Maximum	61.11	149.88	0.87	3.36	1.00	0.99	0.50	0.34	0.99	1.00	3.24	1.56	0.96	0.98	30.56	0.91
Percentiles																
25	31.1450	60.3388	0.7390	1.1810	0.6833	0.9540	0.3992	0.1021	0.9767	0.7830	1.2262	1.1143	0.7919	0.8254	15.6019	0.6272
50	35.1295	74.6135	0.7750	1.2920	0.7740	0.9640	0.4209	0.1201	0.9818	0.8673	1.3246	1.1359	0.8345	0.8689	16.2153	0.6963
75	40.8128	100.3693	0.8050	1.4630	0.8468	0.9710	0.4454	0.1430	0.9854	0.9362	1.4679	1.1630	0.8693	0.9031	16.9973	0.7558

N means the number of samples

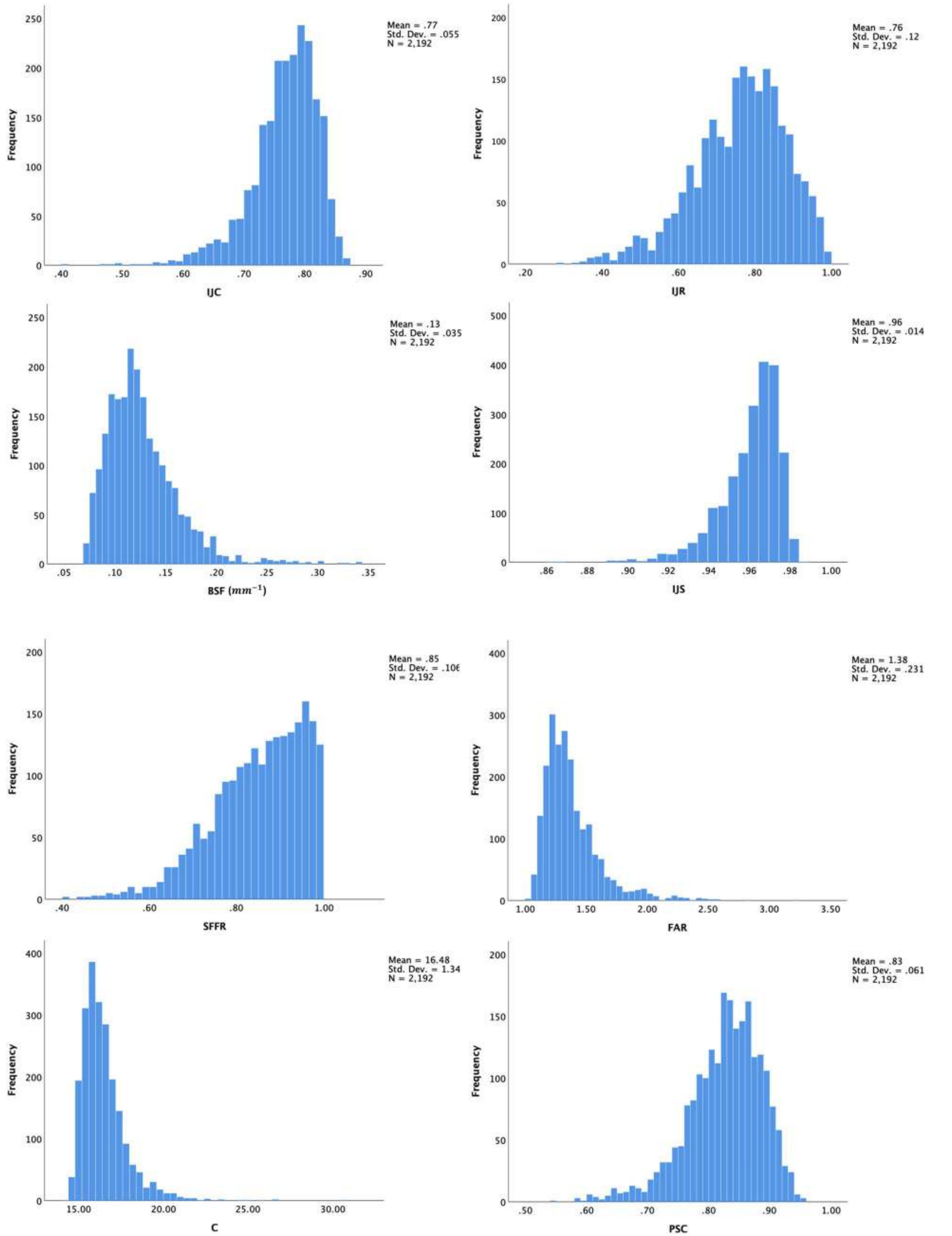

Fig. 6 Histogram distribution of different shape factors

Fig. 7 Frequency vs revolutions distribution

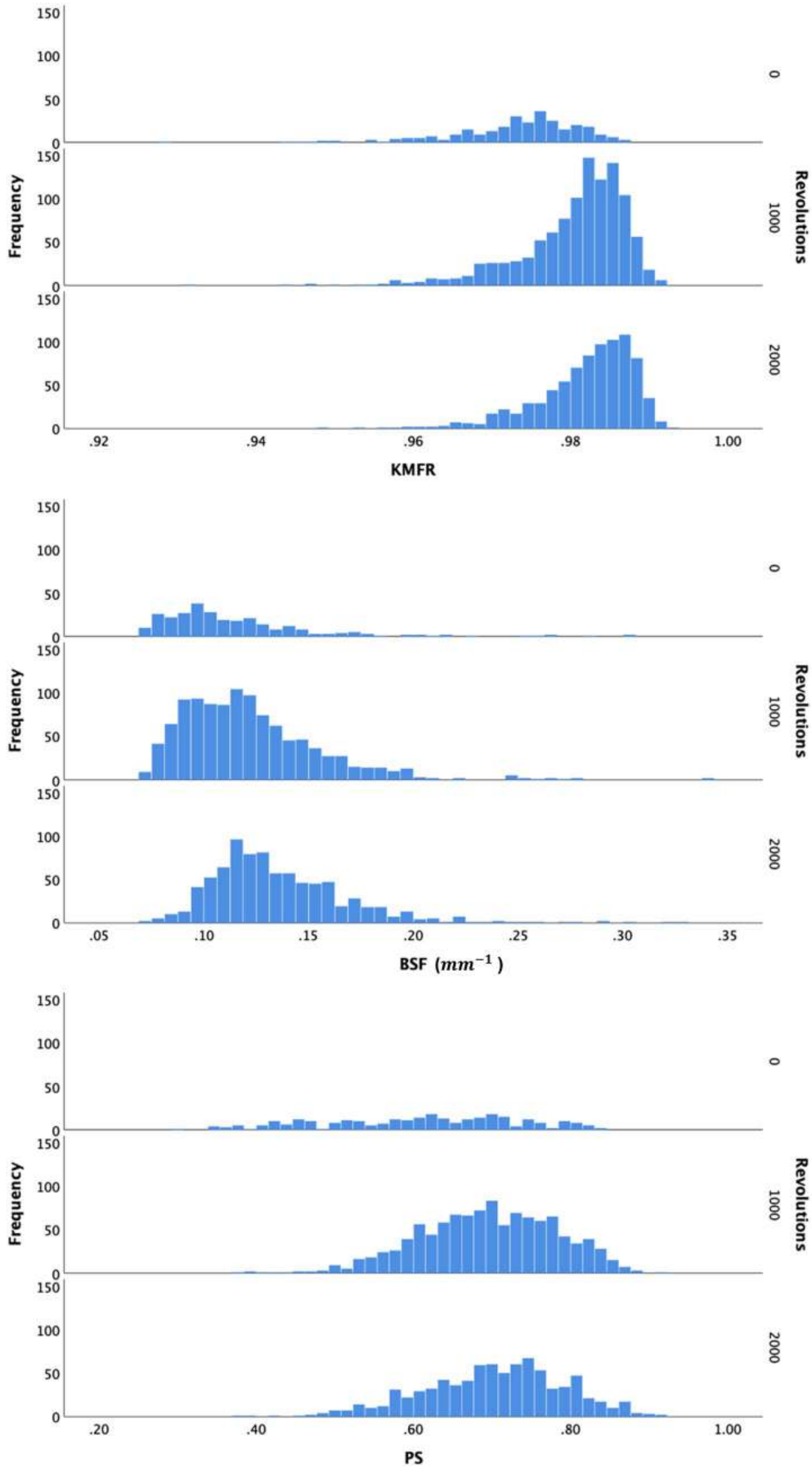

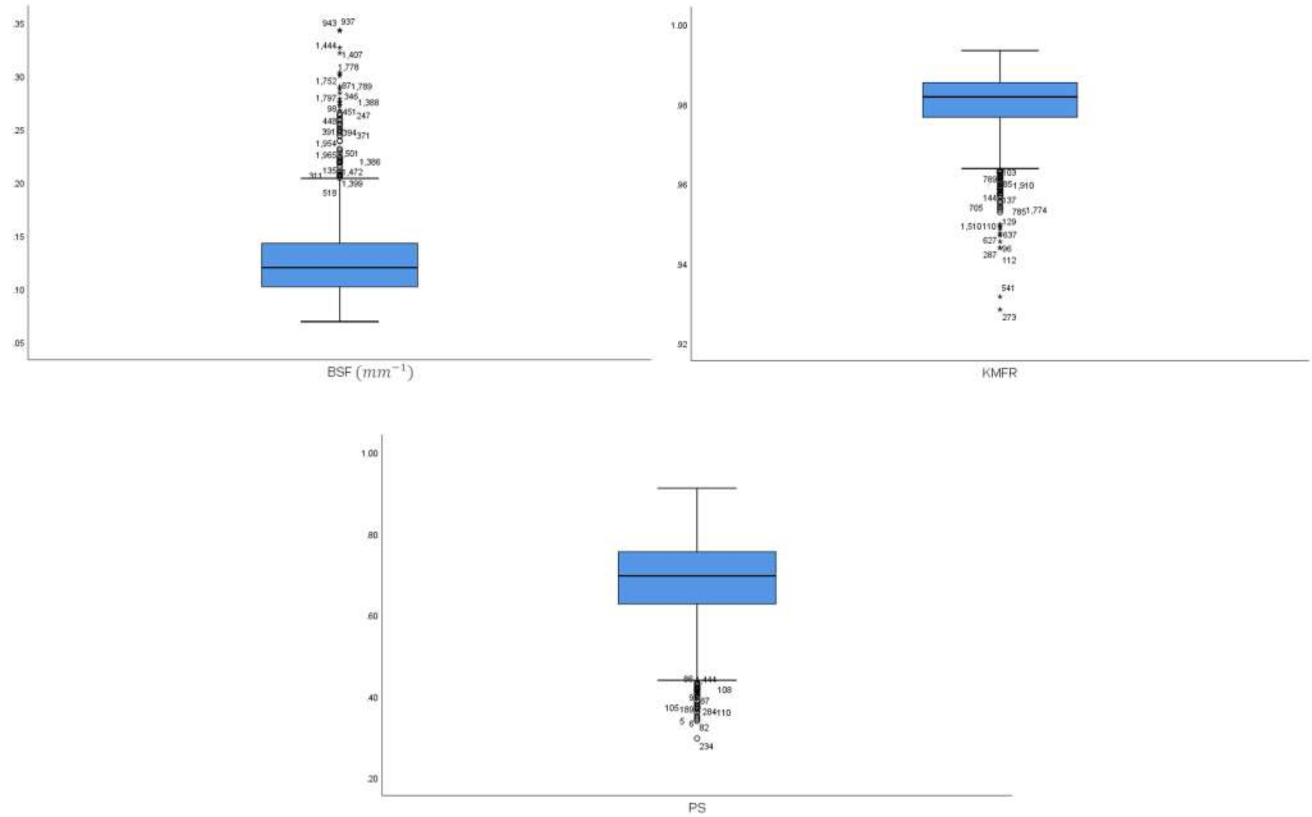

Fig. 8 Box and Whiskers of BSF, KMFR and PS

all revolutions (0, 1000 and 2000). As per the results, it can observe that some of the shape factors show strong correlations (+ 0.95) and some of the factors show very weak correlations.

Perimeter (*P*) and Area (*A*) shows a 0.97 correlation, while PSC & PS, SF & C, and IJS & KMFR show a significant strength of the relationship between two shape factors (1.00), and IJR & ICS, and IJAR & FAR show an (above + 0.95) high correlation. On the other hand, IJC & SF, IJC & C, IJAR & IJR, IJAR & ICS, and FAR & ICS show strong negative correlations (above − 0.95), where the more the variable tends to be on the opposite side of their mean.

Although it can be observed that the IJC & C (− 0.99), IJC & SF (− 0.99), and FAR & ICS (− 0.98) show a nonleaner pattern of their correlation distribution. Probably the two variables are not related linearly. In contrast, the correlation coefficients show a strong inverse linear relationship while plotted data shows a nonlinear pattern. This relationship illustrates why it is important to plot the data to understand relationships that might exist. The selected shape factors correlations further investigate with the number of revolutions (0, 1000, 2000) to see the correlation variation in the milling process. The critical correlations are summered in Table 3.

As per the data shown in Table 3, it can be recognized that there is no considerable variation of correlation coefficients relevant to different LAA revolutions. It can be concluded that milling would not impact the correlations of the shape factors.

Principle component analysis (PCA) was performed to recognize the dimensionality of the data matrix about the total variance in the same shape factors. For the data, it can recognize that only six eigenvalues are more than 1.00, whereas all other PCA shows insignificant eigenvalues lesser than 1. Table 4 shows the variance and cumulative percentages of the total data matrix. It clearly shows a high variance (58.854%) more than half of the total variance. Together these six components show a 99.077% total variance. First, three component shows 90.714% and this indicates that greater than 90% of the variance of the data matrix that had 14 dimensions could be explained with just three dimensions. The rest can be considered as noise in the data and that is lesser than 10%.

Furthermore, PCA analysis data were treated using Varimax with Kaiser normalization to recognize the component loadings (Table 5).

The rotation converged in five iterations and the highest component loadings can be recognized as, IJR, ICS, and FAR showing high loadings (+ 0.9) in component 1 while in

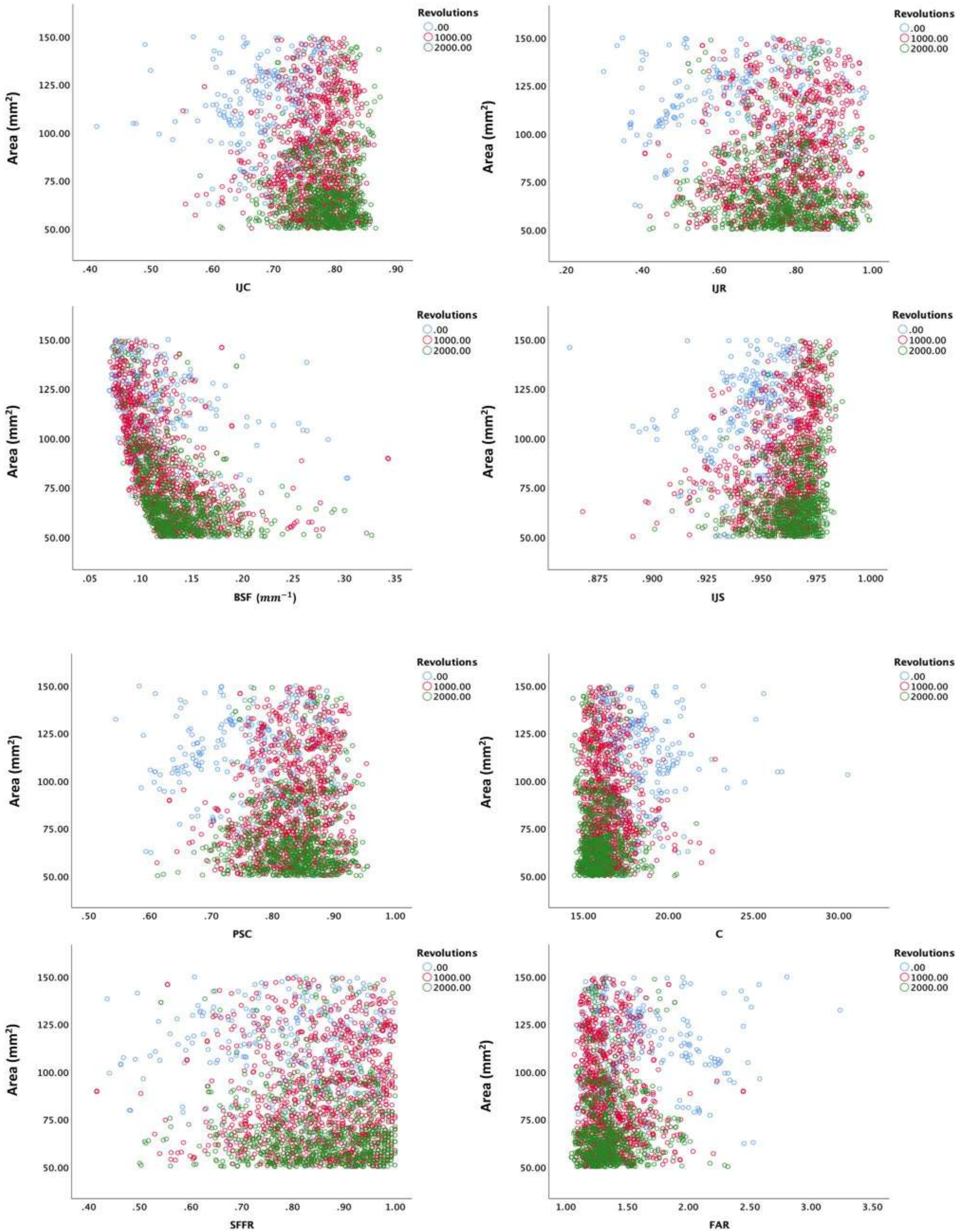

Fig. 9 Shape factor data vs area distribution

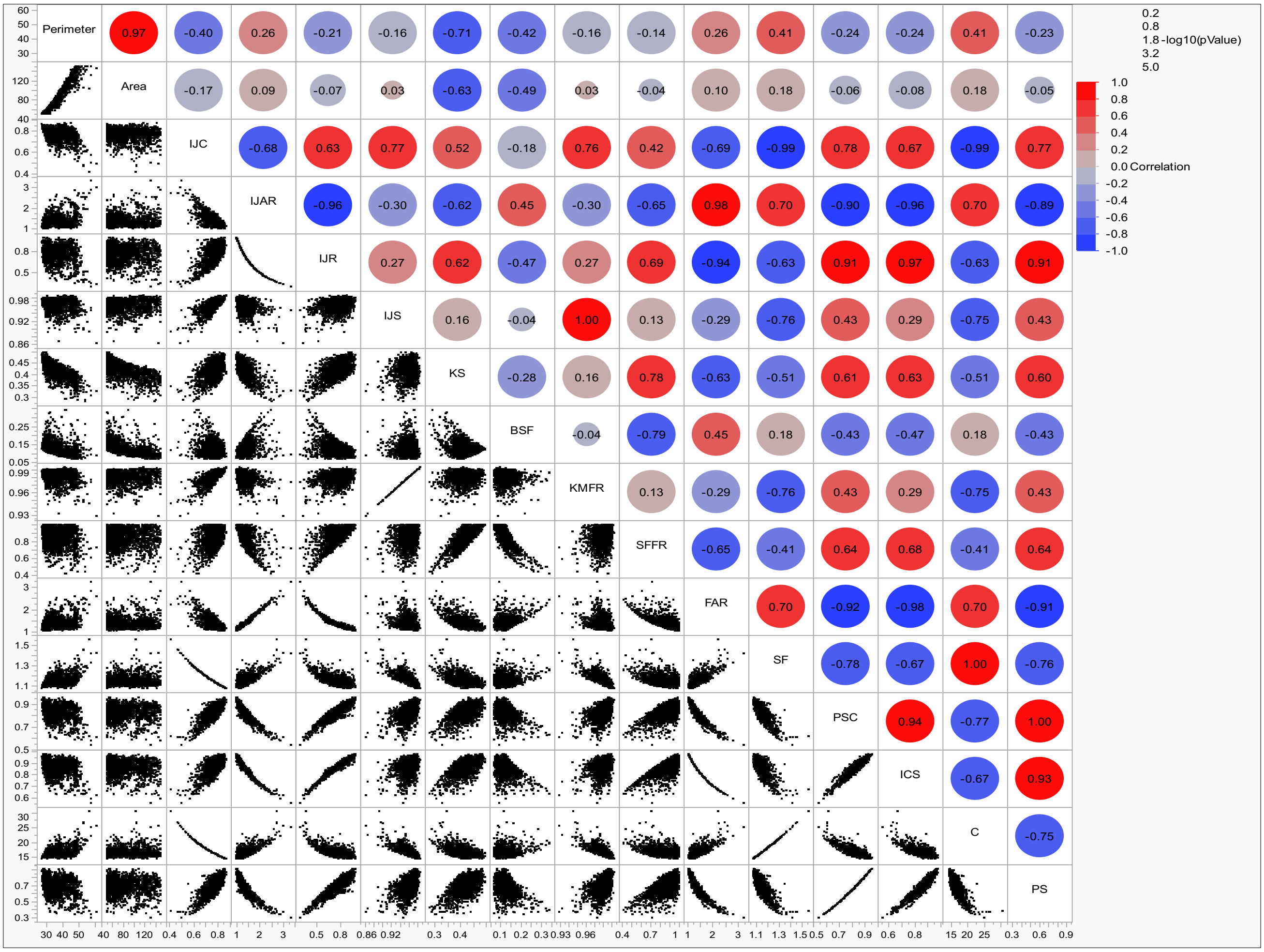

Fig. 10 Pearson's correlation coefficients of all data

Table 3 Pearson correlation summary

Shape factor	Correlation Coefficient		
	0	1000	2000
P and A	0.89	0.97	0.97
PSC and PS	1.00	1.00	1.00
SF and C	1.00	1.00	1.00
IJS and KMFR	1.00	1.00	1.00
IJR and ICS	0.98	0.96	0.97
IJAR and FAR	0.99	0.97	0.98
IJC and SF	−0.99	−1.00	−1.00
IJC and C	−0.98	−0.99	−1.00
IJAR and IJR	−0.96	−0.98	−0.98
IJAR and ICS	−0.97	−0.96	−0.97
FAR and ICS	−0.98	−0.99	−0.99
IJS and BSF	−0.09	−0.13	−0.12
BFS and KMFR	−0.09	−0.13	−0.12

Table 4 Principal component analysis, components, and variance

Component	Variance %
1	58.854
2	17.073
3	14.787
4	5.565
5	1.697
6	1.101

the same component IJAR, SFFR, PSC, and PS show + 0.85 loading. In component 2, IJS and KMFR show high loading and are level at 0.957. Furthermore, it can be recognized that in component 3 there are no cases that can be identified that significantly impact the PCA. Significantly, KS and BSF loadings are low in all three components, and loadings less than 0.4 can be regarded as being small and trivial.

IJC shows a strong negative correlation with SF and C, while IJC is dominant in the second component of the PC (0.822). IJAR strongly correlated with IJR, FAR, and

Table 5 Rotates component matrix

Rotated Component Matrix			
Shape Factor	Component		
	1	2	3
IJC	0.488	0.822	-0.197
IJAR	-0.899	-0.297	0.101
IJR	0.921	0.236	-0.066
IJS	0.053	0.957	0.036
KS	0.687	0.075	-0.611
BSF	-0.683	0.080	-0.547
KMFR	0.053	0.957	0.035
SFFR	0.852	-0.009	-0.005
FAR	-0.906	-0.295	0.104
SF	-0.489	-0.819	0.202
PSC	0.853	0.437	-0.067
ICS	0.926	0.268	-0.084
C	-0.487	-0.815	0.203
PS	0.850	0.429	-0.061

Couples of shape factors that show similar correlations in the component matrix are highlighted in separate colors

ICS while dominant in the 1st PC component with the highest loading (−0.899). Shape factor IJR is strongly correlated with ICS and IJAR, dominant in 1st PC with high loading of 0.921. IJS and KMFR are 100% correlated and dominant in the second component of the PC. KS and BSF show no correlation with other shape factors. In addition, there are no considerable loadings can be observed in the PC. SFFR is not correlated with other shape factors; however, the factor is dominant in the 1st PC component. FAR is correlated with IJAR and ICS and is dominant in the 1st PC component. SF is correlated with IJC and C, further factor is dominant in the second PC. PSC is strongly correlated with the PS and ICS, where the factor is dominant in the 1st component of the PC. ICS is strongly correlated with the IJR, and PS, and negatively in IJAR and FAR, where the factor is dominantly laid in the 1st component of the PC. C is correlated with SF, and negatively with IJC while dominant in the second PC. PS is the 14th shape factor considered in the analysis and PS is strongly correlated with PSC. Further PS is dominant in the 1st PC.

Furthermore, it can be recognized that shape factors IJS & BSF and BSF & KMFR show a weak negative correlation (−0.04), where one variable increase and the other variable tends to decrease, but in a weak or unreliable manner. In addition, it is noticed that KS, BSF & SFFR shape factors do not show a strong correlation with other factors.

3.4 Cluster Analysis from Conventional Statistical Methods

Cluster analysis is used to group similar data into clusters based on the characteristics of all aggregates. The aggregate in size ranges from 50 to 150 mm^2 of projected area. The arrogates belong to 0, 1000, and 2000 revolutions explained in this chapter. The cluster analysis was done on the *z*-scores of the shape factor to avoid bias due to the computed values.

First, Hierarchical clustering is used to identify the number of clusters based on the dendrogram.

Figure 11 shows the dendrogram of the hierarchical cluster analysis, it can identify that the distribution is agglomerative clustering, where each data point has its cluster and iteratively merges the closest pairs of clusters until all data points belong to a single cluster. In addition, illustration can be used to identify the natural groupings of similar data points. It can be used to determine the optimal number of clusters for other clustering algorithms. As per the dendrogram considering sections a–a, it can be recognizing three clusters.

In the constellation plot (shown in Fig. 12) the clusters are shown as branches. This illustration enables better visualization of the relationship between clusters. In addition, plot evidence there are three main branches/clusters.

K means clustering used by pre-defining K as 3 based on the hierarchical cluster finding. The goal of K mean clustering is to minimize the sum of the squared distance between each shape factor data point and its assigned cluster centroid (Table 6).

As per the output, 1208, 829, and 155 data clustered under clusters 1, 2 and 3, respectively. All data are considered valid and no missing data are shown. To identify the cluster membership as a percentage of the total number of aggregates in each milling, cluster membership data were used and presented against the degree of milling.

Figure 13 shows the cluster membership as a percentage of the total number of aggregates in each milling group. As per the illustration, 25%, 58%, and 62% got clustered under cluster 1 against 0,1000 and 2000 revolutions. In addition, it could be observed that a significantly higher percentage of aggregates that had been milled got clustered in the 2nd cluster as opposed to the first cluster. On the other hand, Cluster 2 shows descending pattern in circles with 43%, 38%,

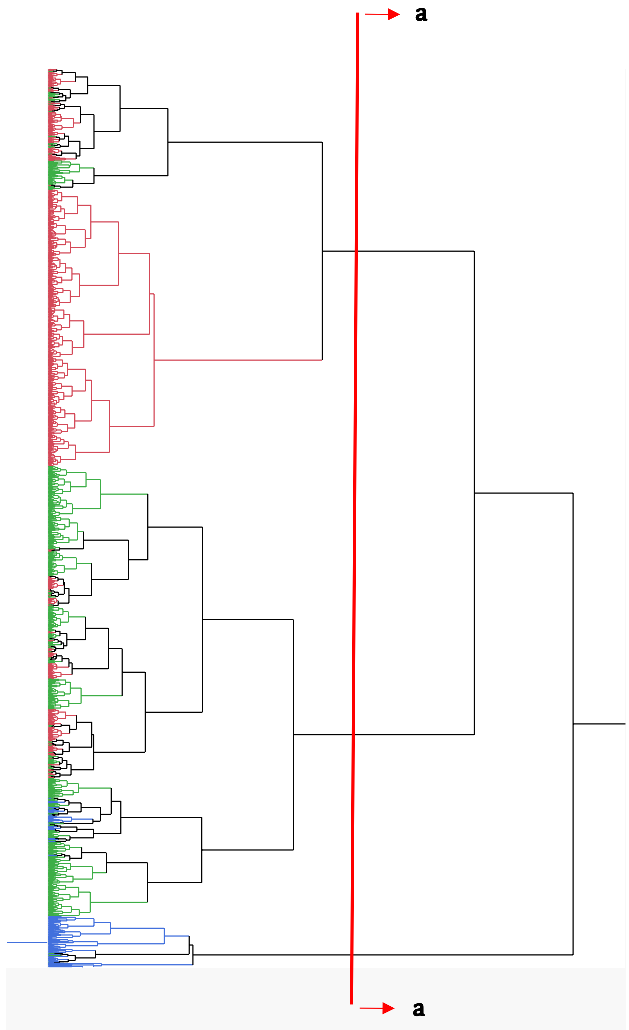

Fig. 11 Hierarchical cluster dendrogram

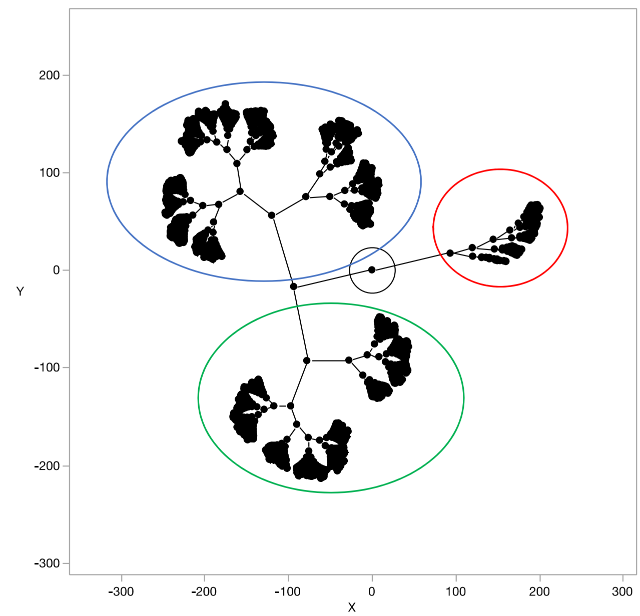

Fig. 12 Cluster constellation plot

Table 6 Number of cases in each cluster

Number of cases in each cluster	
Cluster	
1	1124.000
2	888.000
3	180.000
Valid	2192.000
Missing	0.000

and 35% contributions from 0, 1000, and 2000 revulsions, respectively. However, Cluster 3 shows a light illustration with 32%, 4%, and 3% clusters in 0, 1000 and 2000 degrees of milling. Three clusters did not cluster based on the number of millings. This indicates that the distance between the aggregates computed on 14 shape factors is totally not based variation induced by the process of milling. Moreover, it could be several other aspects of the shape of the aggregate that is distributed within each group of aggregates based on the number of revolutions.

As per Fig. 14, cluster 1 shows law values, while clusters 2 and 3 show extremes of each shape factor. Most of the highest distance centers belong to cluster 3 (above ± 2). In addition, 2nd cluster has the next highest cluster center z-scores of shape factors indicating they are also distinctively distant from each cluster, and it corresponds to aggregates specifically showing the characteristics of originally crushed aggregates with a smaller number of un-milled aggregate contributions. The variation in all three clusters indicates a significant pattern relating to the process of milling.

Figure 15 shows the parallel coordinate plot displaying the structure of the observation in each cluster. Using these plots, it is convenient to understand the difference between clusters. Cluster 1 shows a higher mean, while the mean descends in order clusters 2 and 3, respectively. IJC, IJR, IJS, BS, KMFR, SFFR, PSC, ICS, and PS shows high values in both clusters 1 and 2, while IJAR, BSF, FAR, SF, and C show lower values. Therefore, comparatively, it could be recognizing a similar structure in both clusters 1 and 2. However, it can be observed that different contributions in cluster 3.

Figure 16 shows the plot of the points and clusters in the first three principal components of the data. Circles are drawn around the cluster centers. The size of the circles is proportional to the count inside the cluster. The shaded area is the 50% density contour around the mean (ZScores of shape factors) and indicates, where 50% of the observations

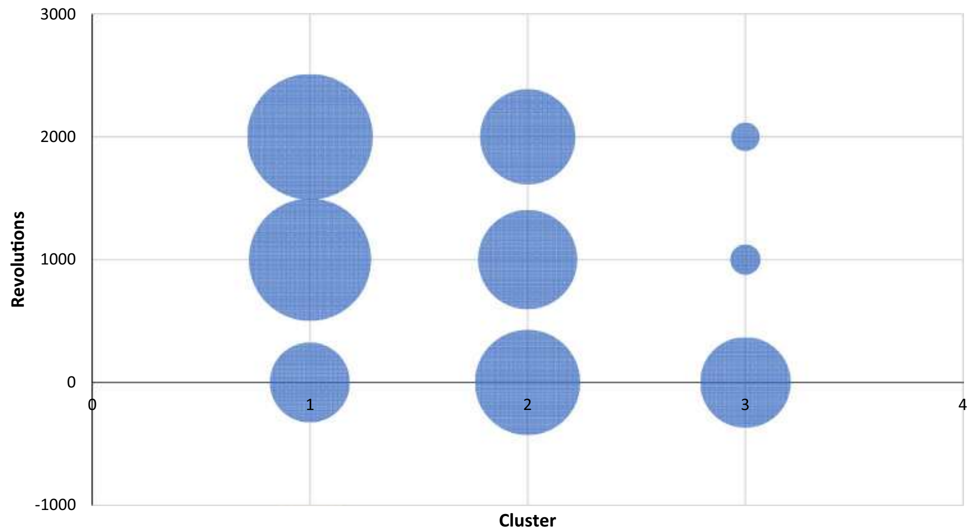

Fig. 13 Cluster membership as a percentage

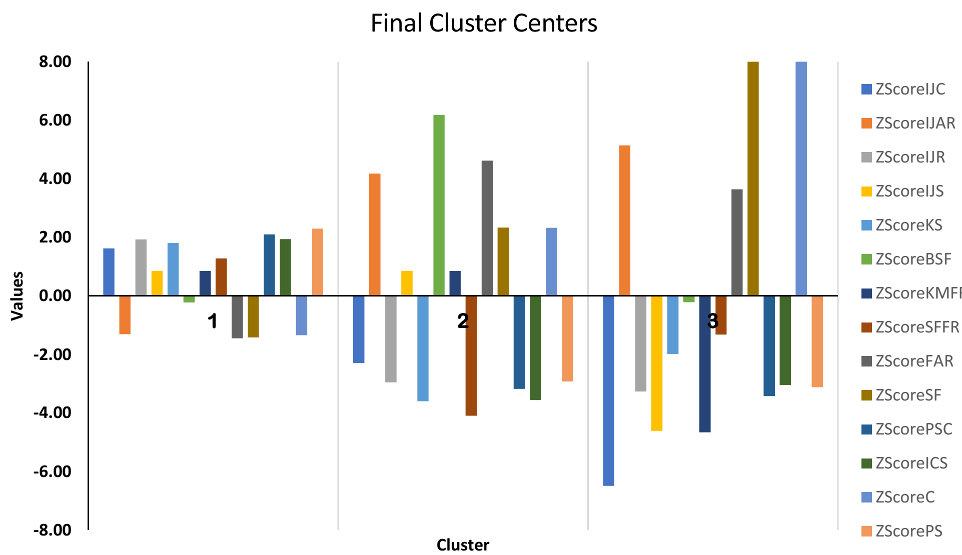

Fig. 14 Plot of final cluster centers

in that cluster would fall. The clusters that appear to be most separated from each other are based on their principal components.

3.5 Geometric Properties Used to Describe the Shape and Characteristics of Aggregates.

Circularity, aspect ratio, roundness, and solidity are all geometric properties used to describe the shape and characteristics of aggregates [25]. While each property focuses on different aspects of the shape, there can be certain similarities and relationships among them. Circularity, roundness, and aspect ratio are all geometric factors that provide quantitative measures of different aspects of the aggregate shape. They help in characterizing the overall form and appearance. Furthermore, circularity, roundness, and aspect ratio are all related to the regularity of the shape. Higher values of circularity and roundness indicate a more regular, symmetrical shape, while lower values suggest irregularity [26]. Aspect ratio specifically measures the elongation or stretching of the shape along a particular axis [27].

3.5.1 Circularity

Regarding the similarities in aggregate shape, these geometric descriptors are all related to different aspects of the shape and can provide complementary information. For example, circularity and roundness both measure the regularity and curvature of the shape, in this analysis IJC and C shape factors describe the circularity in aggregate shape. The c mean value (16.481) is considerably higher than the mean value of IJC (0.7669). In addition, the standard deviation values

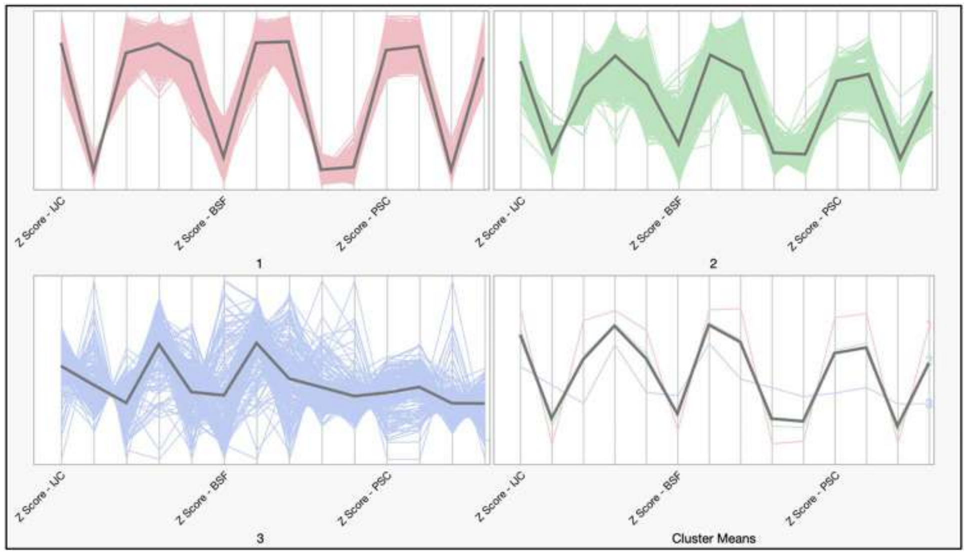

Fig. 15 Cluster—parallel coordinate plot

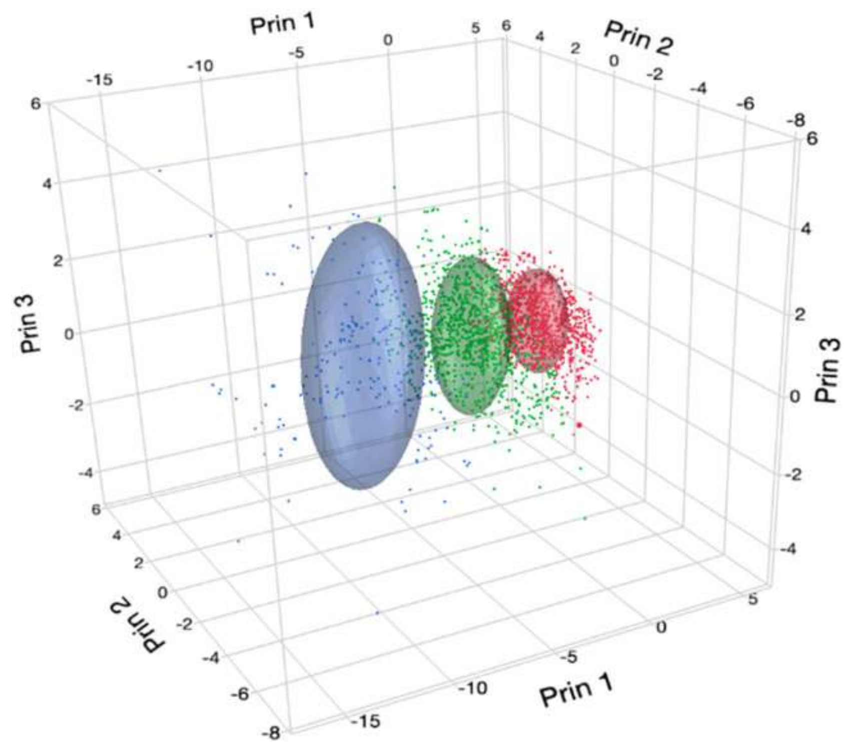

Fig. 16 Plot of the points and clusters in the first three principal components of the data

show greater variability of C (1.34345) comparatively IJC (0.0548). Furthermore, the histogram shows two different patterns of distributions belonging to these two shape factors. IJC shows left skewness (negative), while C shows right (positive). However, from the statistical analysis, it was evident higher correlation of the IJC and C in all milling attempts -0.98, -0.99, and -1.00 in 0, 1000 and 2000, respectively. Furthermore, in PCA analysis, the rotated component matrix indicates both shape factors show high loadings in component 2 ($+0.8$). In addition to that it can identify from the clustering, the highest cluster centers indicated by IJC and C within the 3rd Cluster.

Therefore, considering all the statistical test it can be concluded that IJC and C shows more potential morphological similarities within their quantitative distribution. Circular aggregates tend to pack more efficiently, maximizing the void space between particles. Similarly, aggregates with higher roundness can achieve better packing, reducing voids [28]. Either IJC or C can be used to identify the impact of circularity on the structure of concrete.

3.5.2 Aspect Ratio

The aspect ratio can influence the arrangement of particles in the aggregate, affecting how they pack together. Feret's aspect ratio is another shape factor used to quantify the shape characteristics of aggregates. It measures the elongation or stretching of an object along its maximum and minimum Feret diameters [29]. In this analysis, IJAR and FAR describe the impact of aspect ratio in quantitative analysis. IJAR and FAR show close means (1.355 and 1.378) and medians (1.292 and 1.324). Furthermore, both show similar Skewness (2.066 and 2.009) and Kurtosis values (6.736 and 6.436), from the values it can be imagined that the distribution of both shape factors could be right-hand skewed positive similar distribution of histogram. In addition to the histogram, both factors show an identical distribution in area vs shape factor distribution. From the statistical tests, it is identified that more morphological similarity between these two shape factors. The correlation between IJAR and FAR is possibly strong in all three milling attempts (0.99, 0.97, and 0.98). Further PCA indicates the highest loadings within the 1st component (−0.899 and −0.906). Therefore, it can be concluded that IJAR and FAR homogenously contribute to the analysis and either one of these factors can be used to investigate the impact of aspect ratio in the structure of aggregate packing.

3.5.3 Projected and Inscribed Circle Sphericity

Projected sphericity and inscribed circle sphericity are two measures used to assess the sphericity or roundness of an object or aggregate. While they both relate to the object's shape, they capture different aspects of its roundness. Projected sphericity measures the roundness of an object based on its projection onto a 2D plane. It quantifies how closely the projected shape resembles a circle [30]. Typically, projected sphericity is calculated as the ratio of the area of the object's projection to the area of a circle with the same perimeter as the object's projection. Inscribed circle sphericity, on the other hand, assesses the roundness of an object by considering the largest circle that can be inscribed within it. It measures how well the object's shape can be approximated by a circle. Inscribed circle sphericity is calculated as the ratio of the object's area to the area of the largest inscribed circle [31].

On the other hand, Krumbein sphericity, developed by W.C. Krumbein, is a measurement used to describe the shape of sediment particles. It quantifies how closely a particle approximates a sphere, indicating its roundness. The calculation of Krumbein sphericity involves measuring the longest and shortest axes of the particle and using these dimensions to estimate the surface area [32]. The sphericity value provides a standardized measure to compare the roundness of different sediment particles [31]. Therefore, IJR, KS, ICS, and PS shape factors describe the impact of roundness in an aggregate structure. From that statistics, it can observe that, the means of all factors are not within the same range (0.761, 0.419, 0.859 and 0.687). All four factors show negative skewness and positive Kurtosis values which indicate left skewed histogram distribution; however, PS shows an odd shape compared to the other three factors, it is a kind of bell distribution with a prominent mount in the center and similar tapering to the left and right. Furthermore, by investigating the statistical results it can be recognized that, IJR and ICS show a strong correlation in all three milling attempts. In addition, PS shows a strong correlation with IJR. Therefore, considering the IJR, ICS, and PS it can recognize certain similarities in analysis. The fact justifies the PCA analysis by indicating the highest loading of all three factors under the 1st component. On the other hand, KS does not show a correlation to the other three factors and all other 13 shape factors, and PCA does not indicate concentrate loading on one component. Therefore, it can be concluded that IJR, ICS, and PS shows the similar morphological contribution to the aggregate structure, while KS shows a different impact.

Moreover, PS shows identical similarity with the PSC in the area vs shape factor distribution. Because could check the Pearson correlation, it justifies that PS against PSC is highly correlated (1.00). Both shape factors are laid in the 1st component of the PCA and are identical in cluster distances clusters 2 and 3. Therefore, PSC also shows similar morphological contributions along with IJR, ICS, and PS.

However, the relationship between projected sphericity and inscribed circle sphericity lies in their shared objective of evaluating roundness, but they approach it from different perspectives. Projected sphericity focuses on the 2D projection of the object, examining its planar shape. Inscribed circle sphericity, on the other hand, considers the 2D shape within the object, specifically the largest circle that can fit inside it. Projected sphericity may be more sensitive to elongated shapes that deviate from circularity in their projection, while inscribed circle sphericity is sensitive to irregularities within the object that prevent a tight fit of the largest inscribed circle [33]. Projected sphericity is a 2D measure, capturing the object's roundness when projected onto a plane. Inscribed circle sphericity is also a 2D measure, as it focuses on the shape of the object in a single plane [34].

In general, higher projected sphericity values indicate a closer resemblance to a circle in the object's projected shape. Higher inscribed circle sphericity values suggest a better fit of the object's shape to an inscribed circle, representing a more rounded or spherical object [35]. Therefore, it is important to note that both measures have limitations and assumptions, and their applicability depends on the specific context and requirements of the analysis.

3.5.4 Solidity

Solidity, also known as compaction or density, is an essential property of an aggregate mixture used in construction. The impact of solidity on aggregate mixtures is significant and affects various aspects of the performance and durability of the resulting construction materials. [36]. Solidity plays a crucial role in determining the strength and load-bearing capacity of concrete, asphalt, or other composite materials that use aggregates. Higher solidity generally leads to stronger and more durable structures, as densely compacted aggregates provide better interlocking and resistance to deformation under load. Solidity contributes to the structural stability of a construction material [37]. Adequate solidity ensures that the aggregate particles are tightly packed, reducing the potential for settlement, settling, or shifting of the material over time [38]. This stability is particularly important in applications, such as roads, pavements, and foundations. Solidity affects the permeability and porosity of an aggregate mixture. A higher solidity results in lower porosity which reduces the passage of water and other substances through the material [39]. This is advantageous in applications, where water infiltration can lead to degradation, such as in concrete structures exposed to freeze–thaw cycles. Furthermore, solidity enhances the interlock between aggregate particles, creating a stable matrix within the construction material. This interlock improves the resistance to shear forces and contributes to the overall stability and load transfer capacity of the structure [40]. To optimize the impact of solidity in aggregate mixtures, necessary to carefully select and proportion the aggregates, adjust the compaction methods, and control moisture content during the construction process. By ensuring appropriate solidity, they can enhance the overall performance, strength, and longevity of the resulting construction materials [41].

In this analysis, IJS represents the solidity in an aggregate mixture. According to the statistics, the distribution of the IJS shows negative skewness (− 1.499), while the Kurtosis value is 3.663. Furthermore, the area vs shape factor reveals that IJS and KMFR show identical distribution. Considering the means of IJS and KMFR it can identify that both shape factors show similar distribution in statics. Furthermore, the fact justifies the results of Pearson's correlations analysis. IJS and KMFR show the strongest correlation (1.0) within all milling attempts. Furthermore, PCA analysis indicates the highest loading in 2nd component (0.957). In addition, cluster analysis shows that both shape factors lay in the third cluster with the same cluster distances. Therefore, considering the statistical analysis it can be recognized that both shape factors give an identical outcome against different milling attempts. Therefore, for further analysis either one of these shape factors can be used to recognize the impact of solidity in a mixture of aggregate.

BSF, SFFR, and SF are the remaining shape factors considered for this analysis which was not discussed above, Kawn and Mora have investigated the angularity impact on the aggregate mixture. They have found that several shape parameters have a good correlation with the traditional measure of angularity. Among them, only the convexity ratio and fullness ratio, which are closely related to roundness and angularity, may be taken as measures of angularity [3]. The flatness ratio is a measure of the elongation or flatness of an aggregate particle and is calculated by dividing the minimum dimension of the particle by its maximum dimension. The minimum dimension is typically considered as the smallest width or thickness of the particle, while the maximum dimension is the largest width or length [3]. Sneed and Folk have investigated on flatness ratio impact on an aggerate mixture.

From the statistical investigation, it is difficult to recognize a morphological pattern within these three shape factors. Therefore, it can be recognized that these shape factors individually describe different morphological properties [21]. However, considering KMFR, KMFR shows a strong correlation with IJS (1.0), where IJS describes the impact of solidity. As above discussed, KMFR is identical to IJS and shows statistical similarity in analysis. However, there is no direct similarity between the two concepts. Solidity refers to the compactness or convexity of an object, specifically in the context of its boundary shape. It is calculated as the ratio of the object's area to the area of its convex hull.

SFFR does not show any statistical analysis similarity with the other 13 shape factors, However, SF shows a strong correlation with C (1.0) and area vs shape factor distribution justifies the identical distribution of SF and SFFR. However, PCA shows different placements where C loads in the 2nd Component and SF loads in the 1st Component. This indicates, even though the distribution placements are similar values of both factors are not similar. Furthermore, K means cluster shows similar clusters centered within C and SF, while the contribution is laid in the 3rd cluster. Considering all the facts it can be concluded that either C or SF can be used to identify the aggregate shape impact in terms of circularity in an aggregate mixture.

3.6 Summery of the Discussion

Circularity, roundness, aspect ratio, and solidity are all geometric properties used to describe the shape and characteristics of aggregates. Findings of the analysis are concluded in Table 7.

Table 7 Summery of conclusions under each geometric property

Geometric Property	Findings
Circularity	IJC and C describe the circularity and roundness of the aggregate, where IJC and C show similar statistical distribution and morphological characteristics, where IJC and C can be used to identify the impact of aggregate packing of concrete structure
Roundness	Projected sphericity and inscribed sphericity measure the roundness of an object. IJR, KS, ICS, and PS can be recognized as shape factors that describe the sphericity of an aggregate. Using the data obtained from the correlation analysis, it can be concluded that IJR–ICS and IJR–PS show a strong correlation with each other shape factors. Furthermore, IJR, ICS, and PS show certain similarities that are justified by the PCA analysis. However, KS does not show a similar morphological analysis. On the other hand, KS shows identical similarity with the PSC in distribution as well as in correlation. Therefore, it can be concluded that IJR, ICS, and PS show similar morphological aspects in analysis to understand the impact of sphericity in a mixture of an aggregate
Aspect Ratio	IJAR and FAR describe the impact of aspect ratio in a mixture of aggregate. Based on the statistical analysis it can be recognized that IJAR and FAR homogenously contribute to the analysis and one of these shape factors can be used to identify the impact of aspect ratio in aggregate packing
Solidity	Solidity enhances the interlock between aggregate particles by creating a stable mixture. IJS can be recognized as a shape factor that describes the aggregate shape in solidity. IJS and KMFR show identical outcomes in different milling attempts, where IJS and KMFR describe similar aspects in aggregate solidity
Other	BSF, SFFR, and SF are the shape factors which does not directly explain an aggregate geometry. BSF and SFFR do not show statistical similarity with other shape factors. However, SF shows a strong correlation with SF, and further identical distribution can be observed. In this sense, SF can be used to obtain circularity aspects, where BSF and SFFR independently describe their shape aspects

4 Conclusions and Recommendations

In this paper, aggregate geometric characteristics were investigated and analyzed to identify the possible aggregate shape factors and their statistical relationship. Furthermore, data were used to understand their morphological aspects that are quantified by the shape factors.

5–30 mm in diameter naturally crushed rock particles were used for the investigation. Particles were milled in a ball mill for 0, 1000 and 2000 revolutions to obtain different morphological aspects. The milled aggregate was taken and digital image processing techniques were used to obtain images and data of the aggregate that represent the shape aspects. The following conclusions were made from the analysis.

- During the investigation it was revealed that correlations of the shape factors do not impact the degree of milling. PSC–PS, SF-C, and IJS–KMFR show strong correlations (1.00) in each milling revolution. Furthermore, IJR–ICS and IJAR–FAR show a strong correlation (+0.85), while IJC–SF, IJC-C, IJAR–ICS, and FAR–ICS show a negative strong correlation. Furthermore, it was revealed that KMFR, BSF, and KS do not show any correlation with other shape factors. From the principal component analysis, it was identified that IJAR, IJR, SFFR, FAR, PSC, ICS, and PS shape factors were dominant in component 1. IJCE IJS, KMFR, SF, and C shape factors were dominant in component 2. KS and BSF do not show a significant impact in any of the components, while there are no considerable loadings that can be seen in component 3.
- Circularity, roundness, aspect ratio, and solidity are all geometric properties used to describe the shape and characteristics of aggregates. Based on the statistical analysis the findings are summarized under each geometric property. IJC and *C* shows similar morphological characteristics in teams of circularity. IJR, KS, ICS, and PS can be recognized as shape factors that describe the sphericity of an aggregate. Aspect ratio impact defined by the IJAR and FAR, while IJS and KMFR show identical impact in terms of solidity, BSF, SFFR, and SF do not show any direct aggregate geometry.

The findings of this research will help researchers and practitioners to develop their mix designs considering the impact of aggregate shape on the characteristics and sensitivity of the concrete for targeted applications.

Declarations

Conflict of interest The authors declare no conflict of interest.

References

1. Naija, A., & Miled, K. (2022). Numerical study of the influence of W/C ratio and aggregate shape and size on the ITZ volume fraction in concrete. *Construction and Building Materials, 1301*, 128950.
2. Zhang, Y., et al. (2021). Effects of specimen shape and size on the permeability and mechanical properties of porous concrete. *Construction and Building Materials, 266*, 121074.

3. Kwan, A., Mora, C., & Chan, H. (1999). Particle shape analysis of coarse aggregate using digital image processing. *Cement and Concrete Research, 29*(9), 1403–1410.
4. Anburuvel, A., & Subramaniam, D. N. (2022). A novel multi-variable model for the estimation of compressive strength of pervious concrete. *International Journal of Pavement Research and Technology*. https://doi.org/10.1007/s42947-022-00266-8
5. Arndt, S., Turvey, C., & Andreasen, N. (1999). Correlating and predicting psychiatric symptom ratings: Spearman's r versus Kendall's tau correlation. *Journal of Psychiatry, 33*(2), 97–104.
6. Jamkar, S., & Rao, C. (2004). Index of aggregate particle shape and texture of coarse aggregate as a parameter for concrete mix proportioning. *Cement and Concrete Research, 34*, 2021–2027.
7. Oluwasola, E., et al. (2020). Effect of aggregate shapes on the properties of concrete. *Journal of Civil and Environmental Studies, 1301*. https://doi.org/10.36018/laujoces/0202/50(0110
8. Sajeevan, M., & Subramaniam, D. (2022). Investigation of boundary layer impact on pervious concrete. *International Journal of Pavement Engineering*, 245–250. https://doi.org/10.1080/10298436.2022.2111423
9. Vishlakshi, K., Revathi, V., & Reddy, S. S. (2018). Effect of type of coarse aggregate on the strength properties and fracture energy of normal and high strength concrete. *Engineering Fracture Mechanics, 194*, 52–60.
10. Xu, Z., & Zhou, G. (2023). 3D mesoscale investigation on the compressive fracture of concrete with different aggregate shapes and interface transition zones. *Construction and Building Materials, 393*, 132111.
11. Das, A. (2006). A revisit to aggregate shape parameters. *Material Science.*
12. Rao, C., & Tutumluer, E. (2000). A new image analysis approach for the determination of volume of aggregates. *Transportation Research Record, 1721*, 73–80.
13. Miao, Y., et al. (2019). Feasibility of one side 3-D scanning for characterizing aggregate shape. *International Journal of Pavement Research and Technology, 12*, 197–205.
14. Reyes-Ortiz, O. J., Mejia, M., & Useche-Castelblanco, J. S. (2021). Digital image analysis applied in asphalt mixtures for sieve size curve reconstruction and aggregate distribution homogeneity. *International Journal of Pavement Research and Technology, 14*, 288–298.
15. Gucluer, K. (2020). Investigation of the effects of aggregate textural properties on compressive strength (CS) and ultrasonic pulse velocity (UPV) of concrete. *Journal of Building Engineering, 27*, 100949.
16. Mora, C., & Kwan, A. (2000). Sphericity, shape factor, and convexity measurement of coarse aggregate for concrete using digital image processing. *Cement and Concrete Research, 30*, 351–3580.
17. Ozen, M., & Guler, M. (2014). Assessment of optimum threshold and particle shape parameter for the image analysis of aggregate size distribution of concrete sections. *Optics and Lasers in Engineering, 53*, 122–132.
18. Rueden, C. T., et al. (2017). Image J2: ImageJ for the next generation of scientific image data. *BMC Bioinfomatics*. https://doi.org/10.1186/s12859-017-1934-z
19. Kim, Y., Suh, H. S., & Yun, T. S. (2019). Reliablity and applicability of the Krumbein-Sloss chart for estimating geomechanical properties in sands. *Engineering Geology, 248*, 97–103.
20. Barksdale , R., Kemp, M., Sheffield, W., & Hubbard, J. (1991). Measurement of aggrgate shape, surface area, and rougness. *Transportation Research Record,* 107–116.
21. Lewis, D. W., & McConchie, D. (1994). Textures. *Analytical sedimentology* (pp. 92–129). Boston: Springer.
22. Xu, R., & Di Guida, O. A. (2003). Comparison of sizing small particals using different technologies. *Powder Technology, 132*, 145–153.
23. Cruz-Martias, I., et al. (2019). Spericity and roundness computation for particles using the extream vertices model. *Journal of Computational Science, 30*, 28–40.
24. Zheng, J., & Hryciw, R. D. (2016). Roundness and sphericity of soil particles in assemblies by computational geometry. *Journal of Computing in Civil Engineering*. https://doi.org/10.1061/(ASCE)CP.1943-5487.0000578
25. ASTM C125-15a. (2015). *Standard terminology relating to concrete and concrete aggregate*. ASTM International.
26. Bhat, A. M. (2022). Influence of coarse aggregate shape factors on bituminous mixtures. *International Journal of Engineering Research & Technology (IJERT),* 11(8).
27. Jain, A., Chouhan, J., & Goliya, S. (2011). Effect of shape and size of aggregate on permeability of pervious concrete. *Journal of Engineering Research and Studies, 11*(4), 48–51.
28. Amario, M., Rangel, C. S., Pepe, M., & Filho, R. D. T. (2017). Optimization of normal and high strength recycled aggregate concrete mixtures by using packing model. *Cement and Concrete Composites, 84*, 82–92.
29. Choe, B. (2017). Shape indices and aggregation characteristics of fine aggregates. *Construction and Building Materials, 155*.
30. Pournian, R. M., Shishehbor, M., & Haddock, J. E. (2020). Effects of aggregate shape on the packing density and voids content of asphalt mixtures. *Powder Technology, 363*, 369–386.
31. Bullard, J. W., & Garboczi, E. J. (2013). Defining shape measures for 3D star-shaped particles: Sphericity, roundness, and dimensions. *Powder Technology, 249*, 241–252.
32. Kurumbein, W. C. (1941). Measurement and geological significance of shape and roundness of sedimentary particles. *Journal of Sedimentary Research, 11*(2), 64–72.
33. Gunasekaran, G. & Chandramohan, P., 2018. A comprehensive review of roundness measurement methodologies. *Measurement Science and Technology, 29*(7).
34. Shukla, A., Singh, T., & Ghosh, A. (2016). Comparative study of various methods for roundness measurement: A review. *Measurement, 82*, 189–202.
35. Tsompanakis, Y., & Kalligeris, N. (2004). New roundness indices for the quantitative characterization of the shape of rock fragments. *Journal of Geotechnical and Geoenvironmental Engineering, 130*(11), 1182–1191.
36. Al-Rawashdeh. (2015). Effect of aggregate gradation and compaction on the properties of asphalt concrete pavements. *International Journal of Engineering Research and Technology, 5*.
37. Popovics, S. (2006). *The effect of aggregate properties on concrete. In: Properties of concrete* (4th ed.). Pearson Education Limited.
38. Vazin, H., Zakeri, M., & Vazin, H. (2017). Effect of aggregate gradation variation on the settlement of geogrid reinforced aggregate base courses. *International Journal of Geosynthetics and Ground Engineering, 3*.
39. Al-Otaibi, S. (2016). Influence of aggregate gradation on the porosity and permeability of concrete. *Journal of King Saud University-Engineering Sciences,* 28.
40. Kumar, A., & Bhattacharjee, B. (2014). Effect of aggregate properties on the mechanical properties of high-performance concrete. *Journal of Materials in Civil Engineering, 26*(7).
41. Quiroga, Fowler, P. N., & David, W. (2004). *Effects of aggregate characteristics on performance of Portland cement concrete*. ICAR Technical Reports.

Sathushka Heshan Bandara Wijekoon is currently working as a Ph.D. student attached to the Faculty of Graduate Studies University of Jaffna. He completed his Master, MSc in Structural Engineering from the University of Salford, and his Bachelor's in Civil Engineering from the University of Wolverhampton. Further, he is working as a lecturer in Civil Engineering at the International College of Business and Technology. His research interests are pervious concrete and seismic resilience structural assessments.

Daniel Niruban Subramaniam is currently a senior lecturer attached to the Department of Civil Engineering at the University of Jaffna. He has completed his doctoral degree from Queensland University of Technology, Australia, and MSc from University of Southampton, UK, on water treatment systems. He is an environmental engineer, conducting teaching and research on environmental engineering-related topics, including Water Sensitive Urban Design. His current research interest lies in pervious concrete (as a structural element solution for low-impact development). His other research avenues include water treatment engineering, recycled concrete aggregates, solid waste management, and coastal sediment transport.

Navaratnarajah Sathiparan is currently serving as a Professor in Civil Engineering, attached to Department of Civil Engineering of University of Jaffna. He has completed his Master's and Doctoral Degrees from University of Tokyo, Japan. He is a structural Engineering, conducting lectures and research related to structural engineering and construction materials. His current research primarily lies on sustainable masonry construction materials and pervious concrete.